Cover Page

Universiteit Leiden

Author: Voltan, Stefano
Title: Inducing spin triplet superconductivity in a ferromagnet
Issue Date: 2016-09-29

4

LONG-RANGE PROXIMITY EFFECT INDUCED IN PERMALLOY BY INTRINSIC MAGNETIC INHOMOGENEITY

A possibility, not much explored, for generating triplet Cooper pairs, is to exploit the intrinsic inhomogeneities of ferromagnets with a peculiar magnetic configuration. Permalloy, in particular in its elusive emerging stripe domain (ESD) regime, seems to provide such possibility.

Contents

4.1 Introduction

At the interface between a superconductor (S) and a ferromagnet (F), conventional singlet Cooper pairs can be converted into equal-spin triplet Cooper pairs. Since the triplets have their spins aligned parallel, they are much less affected by the pair breaking caused by the exchange field of the ferromagnet. Thus they can be injected into the F layer and survive for much longer distances compared to the singlets. The phenomenon, extensively described in Chap.1 and Chap.2, is known as long-range proximity effect. The key factor in order to have singlet-to-triplet conversion is the presence of a certain degree of magnetic inhomogeneity at the S/F interface [1]. There are different ways of providing such inhomogeneity. In the original theoretical proposal of Bergeret et *al.* [1], the magnetic inhomogeneity was described in terms of a rotating vector with the angle varying linearly from the S/F interface to the bulk value, within a certain length. This scenario could be realized, for example, in a domain wall within which the magnetization gradually rotates. So far, however, almost all the experiments which provided evidence of a long-range proximity effect relied on different ways to provide the required magnetic inhomogeneity. In most of the experimental works, an extra ferromagnetic layer F' is inserted in between S/F and the inhomogeneity is controlled by varying the collinearity between the magnetization of F and F'. By using holmium (Ho) as F' layer and Co as F layer, Robinson et *al.* [2] more closely reproduced the original theoretical model. Ho, indeed, is a rare-heart ferromagnet with conical magnetic ordering, with the magnetization vector which rotates around the *c*-axis, if we move along it. In this case the inhomogeneity is expected to be intrinsically present in the Ho layer, however the multilayer geometry F'/F/F' is still needed.

In this framework the study of Permalloy (Py = $Fe_{20}Ni_{80}$) is particularly interesting. It is well known that Py, if grown under particular conditions, can form stripe-domains. This is realized when the thickness exceeds a critical value d_{cr}, which depends on the growth parameters such as, amongst others, the deposition rate and the substrate temperature [3–5]. In this configuration the magnetization vector lies in-plane, parallel to the stripe direction in all domains, but alternately deviates upward and downward, as shown in the sketch of Fig.3.1. The out-of-plane component of the different stripes is therefore aligned antiparallel with Neél-domain-walls in between, in which the magnetization rotates coherently. In Chap.3 we extensively described the magnetic properties of Py and we characterized the stripe-domain regime (SD). There, we also showed that below d_{cr} there exists a broad regime, approximately between 0.5 d_{cr} and d_{cr}, where the magnetization is inhomogeneous without being arranged in the stripes. This regime, that we called emerging stripe regime (ESD), is much less de-

fined and not characterized or reported in earlier literature. The intrinsic magnetic inhomogeneity of Py implied in the occurrence of a stripe-domain phase led us to investigate the possibility of using it as possible generator for triplet correlations. The question is whether is possible to have S/F/S (or S/F) structures where the conversion is intrinsically provided by the F layer itself, due to its magnetic configuration, as proposed in Ref. [1].

The research presented in this chapter was initiated at the University of Salerno by K. Ilyina, C. Cirillo and C. Attanasio. The samples to be discussed were grown there, and the critical field measurements on the trilayers (to be presented in Fig.4.1 and 4.2) were performed by the group of Salerno. A report on this can be found in the PhD thesis of K. Ilyina [6]. Data on bilayers were produced jointly. In Leiden, a separate effort was made to produce Py samples withe required stripe domains, but the correct conditions for this were not found.

Below we present the complete picture as it came out of the various measurements. We start with the temperature dependence of the parallel upper critical field, $H_{c2\parallel}(T)$, of simple Nb/Py/Nb trilayers and Nb/Py bilayers. The thickness of the Nb layers, d_{Nb}, is kept constant at 25 nm while the thickness of the Py layer, d_{Py}, is varied across the different thickness regimes: homogeneous (H), emerging stripe-domains (ESD) and stripe-domains (SD). For the trilayer with d_{Py} in the ESD regime, namely for 125 nm $\lesssim d_{Py} \lesssim$ 300 nm, a 2D-3D dimensional crossover (DCO) was observed at $T \simeq 0.9\, T_c$, where T_c is the superconducting critical temperature of the system. Moreover, a clear kink is present in the $H_{c2\parallel}(T)$ curve of Nb/Py bilayers when $d_{Py} = 200$ nm. These observations, which we attribute to an increased effective thickness of the superconducting layer, cannot be explained within the spin-singlet proximity effect, because of the short coherence length, estimated for Py to be about 1.9 nm. The results are rather compatible with a long-range spin-triplet proximity effect, induced by the inhomogeneous magnetic configuration of the ESD regime.

4.2 Sample preparation and measurement methods

Nb/Py/Nb trilayers and Nb/Py bilayers were deposited at the University of Salerno on Si(100) in the same conditions as described in Chap.3, by ultrahigh vacuum dc diode magnetron sputtering at an Ar pressure of 3×10^{-3} Torr after obtaining a base pressure of 2×10^{-8} Torr. The typical deposition rates were 0.25 nm/s for Nb and 0.30

nm/s for Py, measured by a quartz crystal monitor previously calibrated by low-angle x-ray reflectivity measurements on deliberately deposited thin films of each material. The prepared samples are unstructured and the typical in-plane dimensions are about $5 \times 10 \ mm^2$. A schematic of the measured trilayer is shown in Fig.4.1a.

Samples have constant Nb thickness, $d_{Nb} = 25 \ nm$, and variable Py thickness with d_{Py} in the range 20 - 430 nm. Thanks to the presence of a movable shutter in the deposition chamber which selectively covers the substrates, three different samples could be grown in the same deposition run. A single 25-nm-thick Nb film and several single Py films, having the same thickness as the Py layers in the corresponding hybrids, have also been prepared and characterized for comparison.

Single layers of Py were characterized magnetically using Magnetic Force Microscopy (MFM), ferromagnetic resonance (FMR), SQUID magnetometry and magnetoresistance measurements (MR). This characterization has been the aim of Chap.3 so details the used techniques can be found in Sec.3.2.

The resistive transitions of the unstructured multilayers were performed using an in-line four-terminal geometry with a constant bias current of 500 μA. The distance between the current (voltage) pads was about 8 mm (3 mm). The samples, mounted on a copper block and placed at the center of a NbTi superconducting solenoid, were immersed in a He-4 cryostat. During measurements the temperature stabilization was around 1 mK.

4.3 Results

4.3.1 Magnetic characterization

A detailed magnetic characterization of Py as a function of the layer thickness has been presented in Chap.3. Magnetic Force Microscopy (MFM) on unstructured Py single layers (see Fig.3.2) showed that magnetic stripe-domains are visible only above a thickness $d_{Py} \simeq 300 \ nm$, which we defined to be the critical thickness value d_{cr}, i. e. the lower boundary of the stripe-domain regime (SD). For $d < d_{cr}$, two different regimes could be recognized: an homogeneous regime (H), for $d \lesssim 125 \ nm$, and a so-called emerging stripe-domain regime (ESD), for $125 \ nm \lesssim d \lesssim 300 \ nm$. For the samples in the ESD regime, the MFM measurements did not provide evidence of an inhomogeneous magnetic configuration, except for thicknesses close to the transitions to the SD regime. However, signatures of inhomogeneity emerged with other
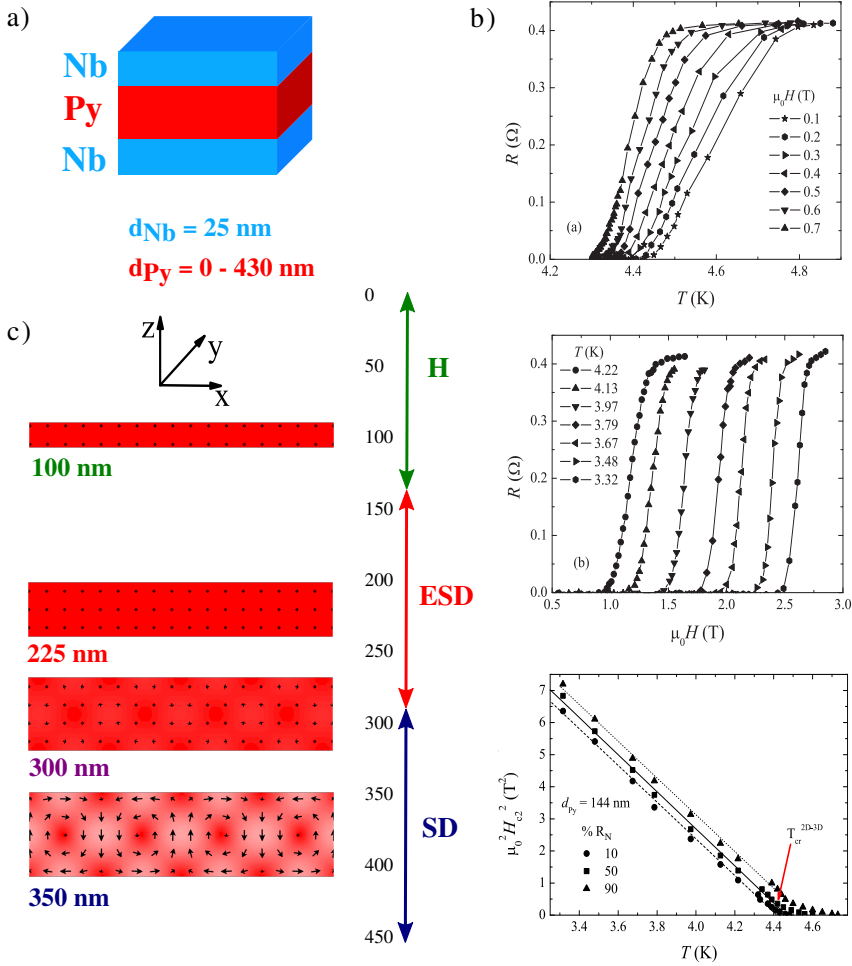
Figure 4.1: (a) Schematics of the measured trilayers. The inner Py layer, whose thickness d_{Py} varies in the range between 20 and 430 nm, is sandwiched between two 25-nm thick Nb films. (b) Resistive transitions for the trilayer Nb(25)/Py(144)/Nb(25). Top panel: $R(T)$ curves at different values of the in-plane applied magnetic field. Central panel: Resistance R as a function of the in-plane field at different temperatures. Bottom panel: temperature dependencies of $H_{c2\parallel}^2(T)$ for the trilayer Nb(25)/Py(144)/Nb(25) determined using three different resistive criteria. The crossover temperature can be easily estimated as the point where the linear fit, which in a quadratic scale identifies the 2D regime, deviates from the experimental data. Data supplied by Ref. [7]. (c) Cross sectional magnetization distribution simulated by OOMMF for four different values of d_{Py}, namely d_{Py} = 100, 225, 300, 350 nm, obtained using the parameters presented in Sec.3.4. The samples are considered to be infinite along the y-axis (2D simulations) with lateral dimension (along x) much larger than the region of interest (6 μm). The arrows schematically indicate the direction of the magnetization component in the xz-plane, while the color show whether the magnetization vector is parallel to the y-axis (red) or it deviates fro it (white). The first indication of inhomogeneities start to be visible for d_{Py} = 300 nm (see arrows); for d_{Py} = 350 nm the stripe-domains are developed.

measurement techniques. That magnetic hysteresis loops $M(\mu_0 H)$ for samples in the ESD regime showed hints of a linear dependence before the saturation was reached. This linear behavior in general is a well-known feature which signals the presence of stripes-domains and it is attributed to the coherent rotation of the stripes before the saturation. The observation of such dependence in the ESD regime, although less pronounced, is an indication of a certain degree of inhomogeneity even if not necessarily in the stripe-form. The tendency of the samples in the ESD regime to have an inhomogeneous configuration emerged more clearly by looking at structured samples, in particular in the domain-wall configuration and in the outcome of magnetoresistance measurements. The domain-wall configuration of the structured samples was reproduced by simulations realized with the object oriented micromagnetic framework (OOMMF) software for all the three different regimes (see Sec.3.4).

In this Chapter the devices of interest are unstructured. For this reason we performed simulations on semi-infinite samples, for different thicknesses. The results are shown in Fig.4.1b. The magnetic parameters used (exchange stiffness constant A, saturation magnetization $M_{\rm s}$ and out-of-plane anisotropy $K_\perp$) are the same as in Sec.3.4. The sample is considered to be infinite along the y- and x-axes while it spans the thickness of the sample along the z-axis. The cross section shown in the figure is thus taken in the xz-plane, while the y-axis points inside this plane and represents the direction along which the sample is initially magnetized, prior to the magnetic measurements. The color code indicates the direction of the magnetization with respect to the y-axis, namely red and white mean the magnetization is respectively parallel or perpendicular to the initial direction. Black arrows indicate the orientation of the components of the magnetization in the xz-plane. The magnetization in the thinnest samples ($d_{\rm Py} = 100$ nm, 225 nm topmost sketches) stay parallel to the initial state (full dark color, indicating an homogeneous magnetic state), while deviations from such state begin to occur at $d_{\rm Py} = 300$ nm, for which areas with magnetization perpendicular to the y-axis start to appear. As $d_{\rm Py}$ increases, the size and density of such areas increase and the magnitude of the component of the magnetization which deviates from the y-axis also grows. At $d_{\rm Py} = 350$ nm (bottom sketch), the domains with an out-of-plane magnetization component have become wide, with thinner domain walls in between. This is the SD regime. From these simulations, thus, no clear evidence of inhomogeneity appear for the ESD regime. However, it is possible that the "semi-infinite" approximation only partially reproduce the real physics of our devices. Furthermore, in the simulations the role of the proximity with superconducting layer is not taken into account. In the study below, the magnetic field is applied parallel to the film plane, and consequently the magnetic flux perpendicular to interface is min-

imum, however the diamagnetic nature of Nb below T_c could influence the magnetic configuration at the interface.

4.3.2 Superconducting transport properties of Nb/Py/Nb trilayers

In order to determine the $H_{c2}(T)$ phase diagrams of the Nb/Py/Nb trilayers, the resistance R was measured either as a function of the temperature T (at a fixed applied magnetic field H) or as a function of H (at a fixed T). The field was applied in-plane, perpendicular to the direction of the bias current. In Fig.4.1b a selection of $R(T)$ and $R(H)$ curves for the trilayer Nb(25)/Py(144)/Nb(25) is presented (numbers in parentheses indicate the thickness expressed in nanometers). T_c has been defined at $T_{50\%}$, namely at the temperature at which the resistance value is 50% of the normal state resistance R_N, measured at $T = 10$ K. Before measuring, a strong magnetic field (approximately 1 T) was applied in the plane of the substrate at low temperatures and then removed. This was done in order to "prepare" the stripes in the SD regime, and for consistency in the other two regimes. The width of the transitions at zero field, defined by $T_{90\%} - T_{10\%}$, is about 200 mK for all the samples and does not increase when a field is applied. The single 25 nm-thick Nb film shows a two-dimensional (2D) behavior ($H_{c2\parallel}(T) \propto \sqrt{1 - T/T_c}$, see Sec.2.1.3), in the whole investigated temperature range and the critical temperature (at zero field) is $T_c \simeq 6.5$ K. The Ginzburg-Landau (GL) coherence length $\xi_{GL}(0)$ has been extracted (see Eq.2.11 and 2.13) from the linear temperature dependence of the perpendicular upper critical field $H_{c2\perp}(T)$: using a nominal thickness of the Nb layer of 25 nm, the obtained value is $\xi_{GL}(0) \simeq 10$ nm, implying a superconducting coherence length $\xi_S(0) = (2/\pi)\xi_{GL}(0) \simeq 7$ nm. This is a normal value for sputtered Nb, where ξ is strongly determined by an electronic mean free path of about 5 nm.

The $H_{c2\parallel}(T)$ phase diagrams for a representative set of the trilayers are presented in Fig.4.2. The samples Nb(25)/Py(105)/Nb(25) (Fig.4.2a) and Nb(25)/Py(430)/Nb(25) (Fig.4.2d) show a 2D-like behavior in the whole temperature range. The black line is the square-root temperature dependence of $H_{c2\parallel}(T)$ obtained leaving $H_{c2\parallel}(0)$ as the only fitting parameter. The first Py thickness is in the H regime, the latter in the SD regime. In both cases, thus, the Nb layer behaves as the isolated single layer. Like in any conventional S/F interface, the singlet component cannot penetrate the Py layer more than 1-2 nm (on both sides), so the Nb layers result isolated. In the (ESD) regime, instead, the behavior is quite different. For both Nb(25)/Py(144)/Nb(25) (Fig.4.2b)
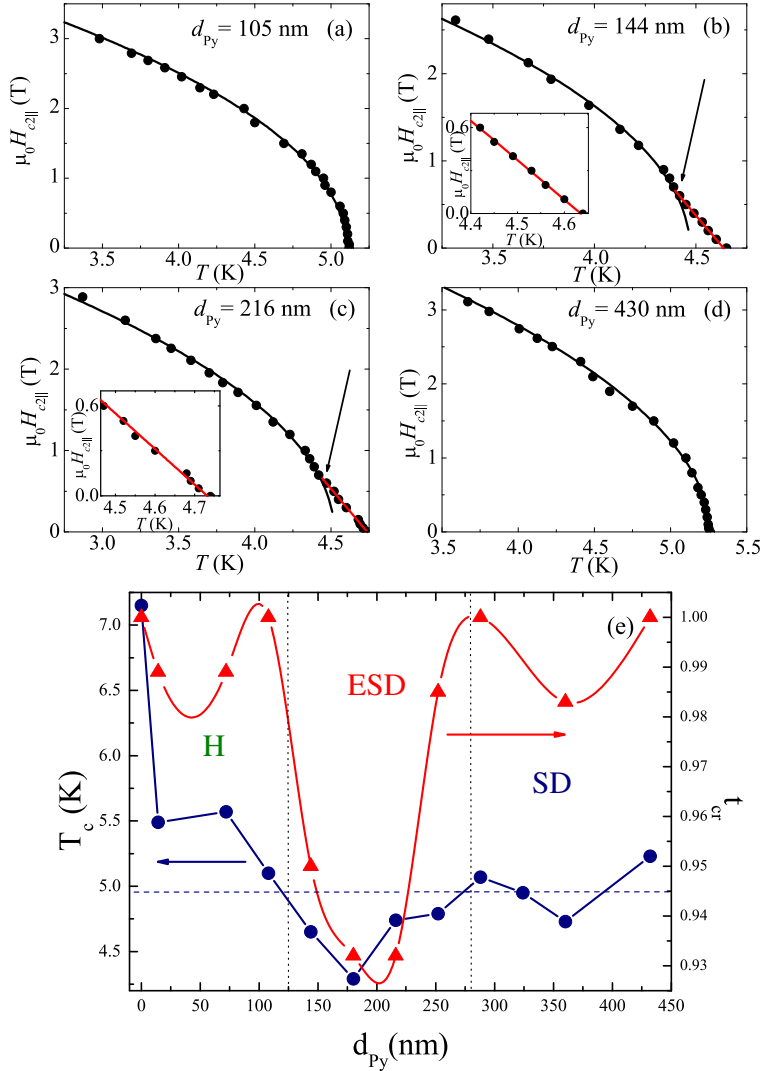
Figure 4.2: Superconducting transport properties and phase diagrams of Nb/Py/Nb trilayers from resistive transitions.(a) $H_{c2}(T)$ phase boundaries of Nb/Py/Nb trilayers with d_{Nb} =25 nm and (a) d_{Py} =105 nm, (b) d_{Py} =144 nm, (c) d_{Py} =216 nm, and (d) d_{Py} =430 nm. Black lines show the square-root (2D) temperature dependence of $H_{c2\parallel}$, that is $H_{c2\parallel}(T) = H_{c2\parallel}(0)\sqrt{1 - T/T_c}$. Red lines show the linear (3D) temperature dependence of $H_{c2\parallel}$, that is $H_{c2\parallel}(T) = H_{c2\parallel}(0)(1 - T/T_c)$. The curves were obtained using $H_{c2\parallel}(0)$ as the only fit parameter. The arrows indicate T_{cr}^{2D-3D}. Insets of (b) and (c): high-temperature region of the corresponding $H_{c2\parallel}(T)$ phase diagrams. (e) ($t_{cr}^{2D-3D} = T_{cr}^{2D-3D}/T_c$) as obtained from $H_{c2\parallel}(T)$ measurements (right scale) and T_c (left scale) as a function of d_{Py} in Nb/Py/Nb trilayers. The red and blue lines are guides to the eye. The dashed vertical lines define the three different regions corresponding to the magnetic configuration (H, ESD, SD) of the Py films. According to the values of t_{cr}^{2D-3D}, in the ESD interval the two outer Nb layers are coupled. Data supplied by Ref. [7].

and Nb(25)/Py(216)/Nb(25) (Fig.4.2c) there is a 2D-3D dimensional crossover (DCO) at a temperature $T_{cr}^{2D-3D} \simeq 0.9 \cdot T_c$. Close to T_c, $H_{c2\parallel}(T)$ is linear, as for a 3D system. At T_{cr}^{2D-3D} this changes to the square-root behavior of a 2D system. The insets in these panels show an enlargement of the data for temperatures close to T_c where the linear behavior of $H_{c2\parallel}(T)$ is much more evident. This indicates a change in the dimensionality of the superconducting layers (in relation to ξ_{GL}) and can be explained within the framework of a long-range proximity effect: the peculiar inhomogeneous magnetic configuration of the ESD layer generates equal-spin triplet Cooper pairs which can "leak" into Py, therefore extending the effective thickness of the superconducting layers. Originally, in Ref. [6], the effect was attributed to the presence of SDs (the ESD regime had not been identified yet) and explained by a coupling between the top and bottom Nb layer across the Py . However, due to the length scales involved, this seems to be very unlikely. The penetration length of the triplet component, indeed, is expected to be limited by the spin diffusion length, ℓ_{sf}, which for Py is relatively small, about 5 nm [8–10], much shorter than the Py thickness. The reason why the 3D-behavior is observed only above T_{cr}^{2D-3D} has to do with the temperature dependence of the coherence length $\xi_S(T) = \xi(0)/\sqrt{1 - T/T_c}$, and it will be more extensively discussed in Sec.4.4. The previous analysis of the $H_{c2\parallel}(T)$ phase diagrams is summarized in Fig.4.2e (right hand scale) where the reduced crossover temperature ($t_{cr}^{2D-3D} = T_{cr}^{2D-3D}/T_c$) is reported for all trilayers. The crossover temperature can be more easily estimated by plotting $H_{c2\parallel}$ vs T, as shown in Fig.4.1b (bottom panel): T_{cr}^{2D-3D} is the value at which the dependence deviates from the linear fit. For values of d_{Py} up to 125 nm (region H) and larger than 300 nm (region SD) t_{cr}^{2D-3D} is essentially equal to 1 (namely there is no crossover) while in the ESD region it is $t_{cr}^{2D-3D} = 0.93 - 0.95$. As a remark, as we show in Fig.4.1b (bottom panel), the choice of the 50% of R_N as a criterion to obtain the $H_{c2\parallel}(T)$ phase boundaries of the different heterostructures does not alter the main results presented above, which are confirmed if the 10% or 90% criteria for the determination of T_c are adopted. In particular, the position of the 2D-3D crossover in the $H_{c2\parallel}(T)$-plane, if present, does not depend on the adopted criterion .

The dependence of T_c (at zero field) on the thickness of Py, plotted in Fig.4.2e (left scale), also shows a clear variation, with a dip in the middle of the ESD regime. Notably, T_c for the trilayer with $d_{Py} = 170$ nm is at least 0.5 K lower than T_c of the trilayers with d_{Py} above 300 nm. This is fully consistent with the explanation for the 2D-3D crossover. When triplets are formed, the leakage of Cooper pairs into the Py layer depletes the superconducting order parameter on the S side of the S/F interface. The length scale of the effect is determined by $\xi_S(0)$ and since the thickness of the super-

conducting layer is only a few times $\xi_S(0)$, the result is a suppression of T_c of the whole layer. The effect has been explained more in details in Sec.2.3.2, when introducing the superconducting triplet spin valve (TSV) effect, and will be encountered again in Chap.5.

4.3.3 Superconducting transport properties of Py/Nb bilayers

Since the observed behavior is expected to be due to two separate S-layers at top and bottom, decoupled from the bottom one by the thick Py layer, a similar effect should be observed for a Nb/Py bilayer. In Fig.4.3 we show the phase diagrams $H_{c2\parallel}(T)$ for Py(d_{Py})/Nb(25) bilayers, with $d_{Py} = 70, 200, 382$ nm. The wires are contacted with
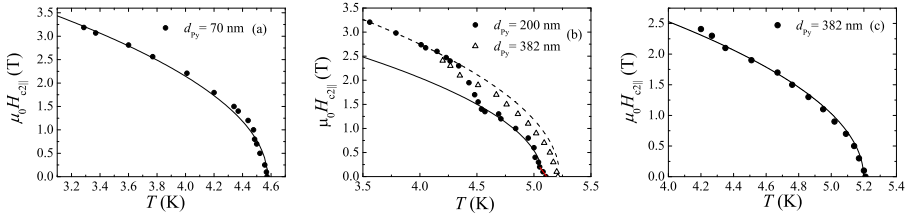

Figure 4.3: Superconducting transport properties and phase diagrams of Nb/Py bilayers. $H_{c2\parallel}(T)$ phase boundaries of Nb/Py bilayers with $d_{Nb} = 25$ nm and (a) $d_{Py} = 70$ nm, (b) $d_{Py} = 200$ nm (closed circles) and $d_{Py} = 382$ nm (open triangles), and (c) $d_{Py} = 382$ nm. Black lines in panels (a) and (c) show the 2D temperature dependence of $H_{c2\parallel}$. Both curves were obtained using $H_{c2\parallel}(0)$ as the only fitting parameter. In panel (b) the red line shows the linear dependence of $H_{c2\parallel}(T)$ near T_c while the solid (dashed) black line shows the square-root dependence of $H_{c2\parallel}(T)$ for temperatures lower (higher) than $T = 4.5$ K.

the top layer, which in this case is Py. This does not affect the outcome of the measurements because at the superconducting transition the main current path is confined within the S layer (plus, possibly, the proximized region) and the wires are basically "extended" down to the normal/superconducting interface. As expected, for $d_{Py} = 70$ and 382 nm (Fig.4.3a and c, respectively; H and SD regime) the dependence is 2-dimensional in the whole temperature range, as for the trilayers. The black lines are the fits of the 2D relation, obtained using $H_{c2\parallel}(0)$ as the only fitting parameter. The bilayer with $d_{Py} = 200$ nm (ESD regime), which in Fig.4.3b is compared with Py(382)/Nb(25), also shows a DCO but in this case the transition is 2D-2D, at about $T = 4.5$ K ($t_{cr}^{2D-2D} \simeq 0.9$). Very close to T_c there is a hint of 2D-3D dimensional crossover, but the small range makes it difficult to judge whether it is a real feature or

an artifact. A possible explanation for the observations is given in Sec.4.4. In this case the variation of T_c is not fully consistent with the model described above. However we have to point out the measured bilayers were grown at different times, and that could account for a variation of the superconducting properties of the Nb layer, due to different sputtering conditions.

4.4 Discussion

The results for the S/F/S trilayers show a 2D-3D dimensional crossover (DCO) in the phase diagram $H_{c2\parallel}(T)$, only when the thickness of the Py layer is in the ESD regime. Such a DCO is typically observed in S/N multilayers [11] (with N a normal metal), and it is ascribed to a change in the dimensionality of the superconducting layer with respect to the coherence length $\xi_{GL}(T)$. This occurs when the thickness d_S of a single layer is lower than (or of the order of) the coherence length (2D regime) but the total thickness of two (or more) layers is larger (3D). When ξ_{GL}, which is temperature dependent, becomes of the order of the spacer length d_N, the S layers are coupled and the $H_{c2\parallel}(T)$ dependence becomes linear (3D-behavior), provided that $d_N < 2\xi_N$. The latter condition makes a DCO unexpected in a S/F multilayer unless d_F is very small [12] or the ferromagnet is diluted [13]. In our case $d_F \gg \xi_F$. For Py, indeed, $E_{ex} \simeq 200$ [14] and the diffusion coefficient can be obtained via the relation $D_F = (1/3)v_F \ell_F$, where v_F is Fermi velocity and ℓ_F is the mean free path. $v_F = 2.2 \times 10^5$ m/s [14] and ℓ_F can be obtained from $\rho\ell_F = 31.5 \times 10^{-6}$ $\mu\Omega$cm^2 [8], knowing that $\rho = 20$ $\mu\Omega$ (value measured at low temperatures). Thus from Eq.1.1, we obtain $\xi_F \simeq 1.9$ nm. The scenario is different if long-range equal-spin triplet Cooper pairs are induced, because of the inhomogeneity in the ESD regime. In this case the coherence length is determined by $\xi_F^T(T) = \sqrt{\hbar D_F/2\pi k_B T}$ (see Sec.2.2.2). By using the value of D_F extrapolated above, at $T = 4.2$ K, $\xi_F^T(T = 4.2$ K$) \simeq 20$ nm $\gg \xi_F(T)$. While estimating the length scale of the proximity effect, also the spin diffusion length ℓ_{sf}, typically the main limiting factor, has to be taken into account. For strong ferromagnets such as Co, ℓ_{sf} is about 60 nm [10, 15], while for Py is expected to be much shorter $\ell_{sf} \simeq 5$ nm [8–10]. Therefore, the possibility that the two Nb layers are coupled across a 200 nm-thick Py layer is extremely unlikely. The DCO in this case seems to be the result of the extended effective S thickness, with only the proximity of the top S/F interface contributing. A similar DCO, indeed, has been observed for a simple Nb/Cu bilayer [16]. Whether the estimated short penetration length, due to ℓ_{sf}, is enough to explain a transition from a 2D to a 3D regime, is unclear. The spin diffusion length for

Py is obtained with a two-current model [17], considering a homogeneously magnetized layer of Py. In the ESD regime, however, there is a certain degree of inhomogeneity which could be responsible for mixing the two channels, resulting in an enhanced effective spin-diffusion length [18, 19].

The observation of a dip in the T_c vs d_{Py} in correspondence of the ESD regime, is a further indication of the origin of the effects being the leakage triplet Cooper pairs into Py. If the suppression of T_c in the trilayer were only due to the leakage of spin-singlet Cooper pairs, the critical temperature values in the studied Py thickness range should be d_{Py} independent, because in this case $d_{Py} \gg \xi_F$. The reason why the triplet generation happens only in the ESD regime, must have to do with the particular inhomogeneity of this thickness region. One could expect that the stripe-domains in the SD regime, and in particular the rotating domain-walls between stripes, could be a source of singlet-to-triplet conversion. However, this is not what the outcome of the measurements suggests. This can be explained by looking at the length scale of the inhomogeneities in this case. The typical width w of the stripes, as shown in Chap.3, is of the same order of magnitude of the thickness d_{Py}, thus $w > 300$ nm, with the domain-wall width δ_w of a similar order of magnitude ($\delta_w \approx 1/3 \cdot w$). This length scale is large, if compared to ξ_F. As a consequence the short-ranged Cooper pairs injected into Py "feel" an homogeneous magnetization and therefore there is no conversion. In the ESD regime, instead, the magnetization is not arranged in stripes. Because of the weak perpendicular anisotropy the magnetic moments have a "tendency" to rotate out-of-plane, and the result is the presence of more localized inhomogeneities. The 3D-2D transition which occurs by lowering the temperature and increasing the magnetic field, is probably due to the alignment of the magnetization which is no longer inhomogeneous. Surprisingly, the transition field ($\simeq 0.5$ T) is an order of magnitude higher than the field of complete saturation (cf. Fig.3.5). A possible explanation could be the presence of unsaturated misaligned moments at the S/F interface, as result of the roughness.

The measurements performed on the bilayers confirm the picture described above, with a DCO observed only for the ESD regime, and at an even higher magnetic field ($\simeq$ 1.5 T). Why the transition in this case is 2D-2D is not entirely trivial. In Ref. [20] a 2D-2D DCO was observed in a Pb/Ge multilayer because the total thickness of the coupled Pb layers are still in the 2D regime. Here, if we fit the $H_{c2\parallel}(T)$ curve of Py(200)/Nb(25) at low temperatures, which coincides with the curve of Py(382)/Nb(25) (see Fig.4.3), we obtain an effective thickness $d_{S_{eff}}$ of about 20 nm. This is also the thickness inferred from the Py(382) data. A lower thickness than the layer thickness is to be expected for an S/F bilayer where strong pair breaking on the

F-side of the interface lowers the Cooper pair density. Close to T_c, instead, the extrapolated $d_{S_{eff}}$ value is approximately 25 nm. On the one hand, this is significantly larger than the low-temperature thickness; on the other, it is thin enough to be in the 2D regime. Maybe even more importantly, the crossover in the $H_{c2\parallel}$-curve of Py(200) suggests that not only the effective thickness decreases, but that also T_c increases, which would be in full agreement with the triplet-leakage scenario. An effective thickness of 25 nm could even be expected to arise from the limits set by the small spin diffusion length. Unfortunately, this is difficult to reconcile with the coupling between the S-layers observed in the trilayers. Both experiments point to the presence of triplets in the ESD regime, but with different length scales. The key here still lies in a better understanding of the inhomogeneous ESD regime, which is not yet available. Barely summing the thicknesses of superconducting and proximized layer can give a qualitative idea but it is a too simplistic analysis. First of all, the extrapolation of the $d_{S_{eff}}$ from $H_{c2\parallel}(T)$ is not completely reliable for a proximized system, where T_c and therefore $H_{c2}(0)$ are modified. In general, the whole picture can better described by saying that in these systems the order parameter adjusts itself, such that it can sustain the highest critical field [21]. The outcome, therefore, is the result of the interplay between parameters such as ξ_S and $\xi_F(T)$ (or $\xi_F^T(T)$), with the magnetic field playing an crucial role in determining the magnetic configuration and thus the (possible) triplet generation.

4.5 Conclusions

To summarize, we showed that equal-spin triplet proximity can be induced in simple Nb/Py/Nb trilayers and Py/Nb bilayer by exploiting the intrinsic magnetic inhomogeneities of Py. The conclusion is indirectly inferred from the dimensional crossover (DCO) observed in the phase diagram $H_{c2\parallel}(T)$. Indeed, the DCO, observed for both tri- and bilayers (2D-3D transition in the first case, 2D-2D in the latter), cannot be described by a short-range singlet proximity. The crossover appears only for Py thicknesses in the emerging stripe-domain (ESD) regime, which seems to provide the optimal degree of inhomogeneous magnetization for the singlet-to-triplet conversion. The interpretation is confirmed by the dependence T_c vs d_{Py} for the trilayers, which shows a strong suppression of T_c in the ESD where the leakage of long-range Cooper pairs is maximum.

BIBLIOGRAPHY

[1] F. S. Bergeret, A. F. Volkov, and K. B. Efetov. Long-range proximity effects in superconductor-ferromagnet structures. *Phys. Rev. Lett.* **86**, 4096 (2001).

[2] J. W. A. Robinson, J. D. S. Witt, and M. G. Blamire. Controlled injection of spin-triplet supercurrents into a strong Ferromagnet. *Science* **329**, 59 (2010).

[3] J. Ben Youssef, N. Vukadinovic, D. Billet, and M. Labrune. Thickness-dependent magnetic excitations in permalloy films with nonuniform magnetization. *Phys. Rev. B* **69**, 174402 (2004).

[4] N. Amos, R. Fernandez, R. Ikkawi, B. Lee, A. Lavrenov, A. Krichevsky, D. Litvinov, and S. Khizroev. Magnetic force microscopy study of magnetic stripe domains in sputter deposited permalloy thin films. *J. Appl. Phys.* **103**, 07E732 (2008).

[5] T. Dastagir, W. Xu, S. Sinha, H. Wu, Y. Cao, and H. Yu. Tuning the permeability of permalloy films for on-chip inductor applications. *Appl. Phys. Lett.* **97**, 162506 (2010).

[6] K. Ilyina. *Electric transport properties of S/F hybrids: weak and inhomogenous ferromagnet.* Ph.D. thesis Università degli Studi di Salerno (2012).

[7] C. Cirillo and C. Attanasio. University of Salerno.

[8] A. F. Mayadas, J. F. Janak, and A. Gangulee. Resistivity of permalloy thin films. *J. Appl. Phys.* **45** (1974).

[9] I. C. Moraru, W. P. Pratt, Jr., and N. O. Birge. Observation of standard spin-switch effects in ferromagnet/superconductor/ferromagnet trilayers with a strong ferromagnet. *Phys. Rev. B* **74**, 220507 (2006).

[10] J. Bass and W. P. Pratt, Jr. Spin-diffusion lengths in metals and alloys, and spin-flipping at metal/metal interfaces: an experimentalist's critical review. *J. Phys. Condens. Matter* **19**, 183201 (2007).

[11] C. S. L. Chun, G.-G. Zheng, J. L. Vincent, and I. K. Schuller. Dimensional crossover in superlattice superconductors. *Phys. Rev. B* **29**, 4915 (1984).

[12] P. Koorevaar, Y. Suzuki, R. Coehoorn, and J. Aarts. Decoupling of superconducting V by ultrathin Fe layers in V/Fe multilayers. *Phys. Rev. B* **49**, 441 (1994).

[13] M. Schöck, C. Sürgers, and H. von Löhneysen. Superconducting and magnetic properties of $Nb/Pd_{1-x}Fe_x/Nb$ triple layers. *EPJ B* **14**, 1 (2000).

[14] J. W. A. Robinson, S. Piano, G. Burnell, C. Bell, and M. G. Blamire. Critical Current Oscillations in Strong Ferromagnetic π Junctions. *Phys. Rev. Lett.* **97**, 177003 (2006).

[15] L. Piraux, S. Dubois, A. Fert, and L. Belliard. The temperature dependence of the perpendicular giant magnetoresistance in Co/Cu multilayered nanowires. *EPJ B* **4**, 413 (1998).

[16] A. Otop, G. R. Boogaard, R. W. A. Hendrikx, M. B. S. Hesselberth, C. Ciuhu, A. Lodder, and J. Aarts. Proximity effects in the superconductor/heavy-fermion bilayer system Nb/CeCu6. *Europhys. Lett.* **64**, 91 (2003).

[17] S. Dubois, L. Piraux, J. M. George, K. Ounadjela, J. L. Duvail, and A. Fert. Evidence for a short spin diffusion length in permalloy from the giant magnetoresistance of multilayered nanowires. *Phys. Rev. B* **60**, 477 (1999).

[18] U. Ruediger, J. Yu, S. Zhang, A. D. Kent, and S. S. P. Parkin. Negative Domain Wall Contribution to the Resistivity of Microfabricated Fe Wires. *Phys. Rev. Lett.* **80**, 5639 (1998).

[19] A. D. Kent, U. Rudiger, J. Yu, L. Thomas, and S. S. P. Parkin. Magnetoresistance, micromagnetism, and domain wall effects in epitaxial Fe and Co structures with stripe domains (invited). *J. Appl. Phys.* **85**, 5243 (1999).

[20] D. Neerinck, K. Temst, C. Vanhaesendonck, Y. Bruynseraede, A. Gilabert, and I. K. Schuller. Crossover in the critical-field of Pb/Ge multilayers from single-film to coupled behavior. *Phys. Rev. B* **43**, 8676 (1991).

[21] T. Nojima, M. Kinoshita, S. Nakano, and Y. Kuwasawa. Transport critical current density and dimensional crossover in superconducting Nb/NbZr multilayers. *Physica C* **206**, 387 (1993).